



Published in final edited form as:

Atmos Environ (1994). 2014 October 1; 95: 142–150. doi:10.1016/j.atmosenv.2014.06.027.

Acetyl Radical Generation in Cigarette Smoke: Quantification and Simulations

Na Hu and Sarah A. Green*

Department of Chemistry, Michigan Technological University, 1400 Townsend Drive, Houghton, MI 49931, USA

Abstract

Free radicals are present in cigarette smoke and can have a negative effect on human health. However, little is known about their formation mechanisms. Acetyl radicals were quantified in tobacco smoke and mechanisms for their generation were investigated by computer simulations. Acetyl radicals were trapped from the gas phase using 3-amino-2, 2, 5, 5-tetramethyl-proxyl (3AP) on solid support to form stable 3AP adducts for later analysis by high performance liquid chromatography (HPLC), mass spectrometry/tandem mass spectrometry (MS-MS/MS) and liquid chromatography–mass spectrometry (LC-MS). Simulations were performed using the Master Chemical Mechanism (MCM). A range of 10–150 nmol/cigarette of acetyl radical was measured from gas phase tobacco smoke of both commercial and research cigarettes under several different smoking conditions. More radicals were detected from the puff smoking method compared to continuous flow sampling. Approximately twice as many acetyl radicals were trapped when a glass fiber particle filter (GF/F specifications) was placed before the trapping zone. Simulations showed that NO/NO₂ reacts with isoprene, initiating chain reactions to produce hydroxyl radical, which abstracts hydrogen from acetaldehyde to generate acetyl radical. These mechanisms can account for the full amount of acetyl radical detected experimentally from cigarette smoke. Similar mechanisms may generate radicals in second hand smoke.

Keywords

free radicals; acetyl radical; isoprene; tobacco smoke; reactive oxygen species; kinetic simulation

1. Introduction

Free radicals are among the many toxic species in tobacco smoke and are implicated in lipid peroxidation, protein oxidation and damage to lungs and other tissues (Ozguner et al., 2005; Pryor, 1986). Radicals in tobacco smoke have been studied since 1958 (Lyons et al., 1958),

© 2014 Elsevier Ltd. All rights reserved.

Corresponding author: Dr. Sarah A. Green, Department of Chemistry, Michigan Technological University, 1400 Townsend Drive, Houghton, MI 49931, USA, Phone: 906-487-2048, Fax: 906-487-2061 Fax: 906-487-2061, sgreen@mtu.edu.

The authors declare that they have no actual or potential competing financial interests.

Publisher's Disclaimer: This is a PDF file of an unedited manuscript that has been accepted for publication. As a service to our customers we are providing this early version of the manuscript. The manuscript will undergo copyediting, typesetting, and review of the resulting proof before it is published in its final citable form. Please note that during the production process errors may be discovered which could affect the content, and all legal disclaimers that apply to the journal pertain.

but the mechanisms of their formation have remained elusive because of their transient nature and the chemical and physical complexity of smoke (Borgerding and Klus, 2005; Polzin et al., 2007; Stabbert et al., 2003a; Stabbert et al., 2003b) (Huang et al., 2005; Maskos et al., 2008). Surprisingly, inconsistent with their highly reactive nature, free radicals are detected well beyond the burning site, even as long as 10 minutes post combustion (Cueto and Pryor, 1994; Flicker and Green, 1998, 2001; Pryor et al., 1993). To explain this paradox, Pryor et al. (Pryor et al., 1993) proposed that radicals are continuously formed and destroyed in the gas phase by a so-called steady state mechanism based on the addition of NO₂ to alkylidienes. However, recent studies have raised questions about this mechanism because of the lack of evidence for NO₂-containing radicals and the discovery of apparently unrelated radicals, such as alkylaminobocarbonyl and acyl radicals in mainstream smoke (Bartalis et al., 2007; Bartalis et al., 2009). In addition, several studies have indicated that use of a filter to separate gas phase smoke from total particulate matter (TPM) substantially influences the generation of radicals (Wooten, 2011). In this paper, we investigate three possible mechanisms for the formation of acetyl radical in gas phase smoke: (i) formation by hydrogen abstraction from acetaldehyde by NO₂, which is generated by the oxidation of NO; (ii) additional chain reactions following the initial acetaldehyde/NO₂ reaction; (iii) chain reactions that include isoprene, in addition to NO and acetaldehyde.

Mainstream smoke, sometimes called whole smoke, is the aerosol gas mixture generated during a puff from the burning site drawn through the cigarette rod, and inhaled by the smoker. Sidestream smoke is primarily formed at lower temperatures between puffs during the smoldering process. Both mainstream and sidestream smoke contain a myriad of organic compounds in non-equilibrium conditions and distributed between gas and particulate phases. The fraction of smoke collected on a glass fiber filter is defined as total particle matter (TPM), while the fraction passing through is defined as the gas phase (Baker, 1999). Here we focus on the generation of acetyl radical in mainstream smoke and compare whole smoke to gas phase smoke.

2. Methods

2.1 Chemicals

3-amino-2, 2, 5, 5-tetramethyl-proxyl (3AP), naphthalene-2, 3-dicarboxaldehyde (NDA), sodium cyanide, cyclopentylamine (CPA), and HPLC grade methanol were purchased from ACROS. All chemicals were of the highest purity available and were used without further purification. Since cigarette design varies from brand to brand (Thompson and Mizaikoff, 2006) and human smoking behaviors are very personal and inconsistent, two types of cigarettes, Marlboro and 3R4F Kentucky Reference, were investigated under two different smoking conditions to provide a general picture of radicals generation in tobacco smoke. Marlboro brand cigarettes were purchased from a local vendor and 3R4F Kentucky Reference cigarettes were purchased from University of Kentucky, Lexington (Davies and Vaught, 1990). These cigarettes were 84 mm long, weighing 1.06 g with filter length of 27 mm. A detailed description of this cigarette has been reported (Davies and Vaught, 1990). Solutions of NDA in acetonitrile (10.0 mM) and sodium cyanide solutions (10.0 mM) were

prepared every two weeks and stored at $-5\text{ }^{\circ}\text{C}$. Water used for all solutions was from a Millipore Milli-Q system.

2.2 Experimental Procedures

2.2.1 Smoke—A solution of 0.05 g 3AP in a small amount of acetone was coated on the inner wall of the 140-mL sampling column (30 cm, id 2.6 cm) and dried by rotary evaporation at room temperature. For the continuous draw method, a pump with flow rate 0.6 L/min drew smoke through the column, giving a residence time of about 15 s (Fig S1). Comparison experiments employed the FTC smoking methods, which consists of a 35 mL puff volume drawn over 2 second duration once per minute. By employing the FTC smoking method, one puff of smoke remained in the trapping column and tubing for 250 s. Five Marlboro or 3R4F Kentucky Reference cigarettes were smoked sequentially for each analysis. Experiments were conducted with either whole smoke (manufacturer's integral filter only) or with an additional glass microfiber filter (GF/F, Circles, 25 mm diameter, Whatman[®]) to select gas phase smoke. Temperature and room humidity were ambient. (The ambient temperature is between 20 – 25 $^{\circ}\text{C}$ and the relative humidity between 40 – 60 %). Humidity and temperature of the compressed air were not controlled.

2.2.2 Model Gas—A model system was employed to assess the gas-phase reaction of NO_2 and CH_3CHO . Air from building supply was flowed across liquid phase acetaldehyde at room temperature to carry gas phase CH_3CHO to a Y- junction where it met 1000 ppm NO (certified 1003.1 ppm, Praxair Distribution Inc.) in N_2 (Figure 1). The combined flow rate for NO and CH_3CHO was 0.35 L/min and the residence time from the mixing point through the column was 25 s. As NO mixed with the air, it was oxidized to NO_2 , producing a distinctive brown color. A distillation column coated with 3AP on the inner wall acted as the reaction vessel and trapping surface. Radicals generated within the column were trapped by 3AP.

2.2.3 Analyses—Cigarette smoke experiments were conducted under both Federal Trade Commission (FTC) puff conditions and a pump-drawn continuous flow method, with or without a filter. Two different types of cigarettes, Marlboro and 3R4F Kentucky Reference cigarettes were sampled by each smoking method. A gas mixture consisting of nitric oxide, air and acetaldehyde was employed as a simplified model to mimic the gas phase reaction in cigarette smoke.

Based on previous work (Flicker and Green, 1998, 2001), we adopted a solvent-free radical trapping method to trap carbon-centered radicals. We modified the bead trapping method by directly coating the trapping agent, 3-amino-2, 2, 5, 5-tetramethyl-proxyl (3AP), onto the inner wall of a distillation column to reduce the effect of total particulate matter (TPM) trapped by beads. Smoke from a burning cigarette, or the gas mixture in the model system, flowed through the column; 3AP reacted with the carbon-centered radicals to form stable 3AP adducts, which were then either identified by LC-MS or, for quantification, derivatized with naphthalene-2, 3-dicarboxaldehyde (NDA) as shown in Scheme 1 below. The derivatized adduct was then detected by HPLC/FLD or ESI-MS.

3AP adducts (R-3AP) were washed from the trapping surface with 10 mL methanol. The solution was passed through a Hyper Sep C18 column (Thermo Electron Corporation®) to remove tar and other components, and flushed out with 10 mL methanol to give a dark yellow solution. For derivatization, 500 μ L of water, 500 μ L of filtered sample solution, 200 μ L of sodium cyanide solution, and 200 μ L of NDA solution were added sequentially to a foil-wrapped glass vial and allowed to react for 30 min.

After derivatization, the 3AP adduct solution was filtered with a 0.2- μ m syringe filter (Alltech®); some of the R-3AP-NDA remained on the filter as a yellow precipitate. The precipitate was washed off with 1 mL 20:80% v/v H₂O:methanol and combined with the filtered solution for injection into the HPLC.

Standard adducts of acetyl radical were made photochemically; 3AP (0.5 mM) and acetone (50 mM in water) were irradiated in a 1-cm quartz cell with a 150-W xenon lamp for 30 min. Oxygen competition with 3AP was minimized by flushing the solution before and during irradiation with N₂ (99.99%, Praxair Distribution Inc.). Acetyl radical was identified and quantified as its 3AP adduct by high-performance liquid chromatography with fluorescence detection (HPLC-FLD) analysis, electrospray mass spectrometry (ESI-MS), tandem mass spectrometry (MS/MS), and liquid chromatogram mass spectrometry (LC-MS). In addition to the experimental investigations, computational simulation by Matlab and the Master Chemical Mechanism (Saunders et al., 1997, 2003) were employed to study the kinetics of the proposed mechanisms.

2.3 Instrumentation

2.3.1 HPLC—The HPLC was a Shimadzu Prominence LC-20AD with DGU-20A₅ vacuum degasser, Shimadzu SPD-20AU UV/Vis detector, RF-10A_{XL} fluorescence detector (FLD), Thermo BioBasic-18125 \times 4mm 5 μ particle-packed column; the injection volume was 20 μ L. The FLD was operated at 420/480 nm excitation/emission wavelengths for all separations. Separations of R-3AP-NDA adducts were carried out isocratically at 25°C, with a flow rate of 0.500 mL/min. The mobile phase composition was 30:70% v/v H₂O/methanol.

A stock solution of 10 mM CPA was used to make a calibration curve to estimate concentrations of trapped radicals. CPA acts as an analog for 3AP in the reaction of its primary amine group with NDA; because CPA, like R-3AP, lacks the quenching nitroxide group, there is no reason to expect that the fluorescence yields of CPA-NDA and R-3AP-NDA differ substantially. CPA was derivatized by NDA as above, sequentially diluted and used as an external standard for quantitative analysis.

2.3.2 Mass spectrometry—Mass spectrometric analyses were conducted with a Thermo Finnigan LCQTM Advantage LC/MS. The mobile phase was 50:50% v/v methanol/H₂O with 0.2% acetic acid; the HPLC column was the same as above. The flow rate was 0.200 mL/min. Ionization conditions were capillary voltage 3.95 kV, cone voltage 35 V, sheath gas flow 29.00 L/min, auxiliary gas flow 49.47 L/min, capillary temperature 252.30 °C, ND collision potential 20 V. Selected ion monitoring (SIM) was employed to detect 3AP-C (O) CH₃ (m/z 200.15).

2.4 Computations

Publically available Matlab routines (Brook, 2005; ERI, 2010) were employed to run simplified kinetic calculations of the generation of acetyl radicals from model gas mixture and cigarette smoke. More complex chain reaction simulations employed the Master Chemical Mechanisms (MCM) program from Leeds University, which was designed for atmospheric chemistry (Saunders et al., 1997, 2003). Modeling focused on the trapping experiment in which the smoke was at room temperature. It is not yet feasible to model evolving temperature gradients in smoke. (For modeling details see Supplemental Material.)

3. Results

Representative chromatograms of fluorescent radical adducts trapped from smoke of Marlboro and 3R4F cigarettes under different smoking conditions, with or without a particle filter, and from the model gas mixture are shown in Figure 2(a).

In Figure 2(a), each fluorescent peak in the normalized chromatograms corresponds to a different trapped carbon-centered radical. The peaks were normalized to the strongest signal for better display. The major peak in all smoke samples and the gas mixture corresponds to the acetyl radical (at 6.3 min), matching the peak resulting from acetone irradiation. The chromatogram from cigarette smoke indicates the presence of at least 7 major and several minor radicals. The model gas mixture also shows several peaks in addition to the acetyl radical. The double peaks around 14 min corresponds to oxidized 3AP adducts (Jia et al., 2009).

A blank control containing only NDA-derivatized 3AP showed negligible fluorescence background. For quantitative analysis, NDA-derivatized cyclopentylamine (CPA-NDA), eluting at 7.1 min, was employed as an external standard. Five standards were run by HPLC, yielding a linear calibration curve with a correlation coefficient of 0.972. (Supplemental Material, Figure S2). The highest concentration at 148 nmol/cig was from the 3R4F Kentucky Reference cigarette with a GF/F particle filter under FTC smoking condition, while the lowest at 10 nmol/cig was from the Marlboro continuous drawn sample without a particle filter (Figure 2(b)).

The unambiguous detection of the acetyl radical in cigarette smoke was confirmed by electrospray ionization mass spectrometry (ESI-MS) and tandem mass spectrometry (MS/MS) shown in Figure 3. LC-MS of samples without NDA derivatization further confirmed the presence of acetyl radical adducts in tobacco smoke and model systems (Figure S3).

ESI-MS spectrum of the smoke sample shows the $[M+1]^+$ peak of $\text{CH}_3\text{C}(\text{O})\text{-3AP-NDA}$ at m/z of 376.39 as the most abundant peak (Figure 3, Left). Collision-induced dissociation (CID) of this peak in the tandem mass spectrometer, revealed a loss of the methyl group (-15) (Figure 3, Insert). The same mother peak and fragmentation were observed from the model system and from radicals resulting from acetone photolysis. Selected ion monitoring (SIM) by LC-MS shows that the ion range of 200.6–201.6, corresponding to the $[M+1]^+$ peak for $\text{3AP-C}(\text{O})\text{CH}_3$ from all the three samples eluted at about 3.7 min, as shown in

Figure S3. Thus, the presence of $\text{CH}_3\text{C}(\text{O})\cdot$ in smoke and gas phase model has been confirmed by a variety of analytical techniques, specifically (i) HPLC-Fl of NDA-3AP-C(O)CH₃; (ii) MS/MS of NDA-3AP-C(O)CH₃; (iii) LC-MS of 3AP-C(O)CH₃.

4. Discussion and Simulations

Several immediate conclusions can be drawn from our experimental results. First, the major carbon-centered radical detected was the acetyl radical with 10–150 nmol/cigarette, found in both types of cigarettes and all conditions investigated. Second, more acetyl radicals were generated by the FTC puff-resolved method than by the continuous draw method. Third, under the same FTC smoking conditions, both Marlboro and 3R4F cigarettes produced more acetyl radicals in the presence of a GF/F particle filter.

Pryor and coworkers (Pryor et al., 1983a) first suggested that the production of carbon-centered radicals in smoke is closely related to NO_x reactions, and that NO from cigarette smoke could be oxidized to NO_2 during and after the burning process. That early work proposed that NO_2 could react with species such as alkenes and dienes to produce carbon-centered radicals (Pryor et al., 1983b). Several efforts have been made to mimic the generation of radicals in gas mixtures consisting of NO, air, and other species, such as isoprene (Pryor et al., 1983a), and with methanol as an OH scavenger (Flicker and Green, 2001). However, no direct evidence has been shown for this reaction and the expected NO_2 addition products have not been found.

4.1 Simplified $\text{NO}-\text{NO}_2-\text{CH}_3\text{CHO}$ Mechanism Investigation by Matlab

To better understand how acetyl radicals are generated, we used a computational simulation to investigate a series of reactions in gas phase as shown in Table 1. Reactions were selected from the NIST database based on the concentrations of smoke constituents and relative reaction rates. Our specific goal was to identify the key precursors and reaction pathways that produce this primary radical. We first consider mechanisms based on NO and acetaldehyde, both of which are major components of smoke.

As in previous studies, the reactive species is taken to be NO_2 , which is slowly produced by oxidation of NO in the plume (Reaction 1). In a second step, NO_2 abstracts hydrogen from acetaldehyde to give the acetyl radical (Reaction 2). As one of the major components in tobacco smoke ($900 \pm 250 \mu\text{g}/\text{cig}$) (Borgerding and Klus, 2005), acetaldehyde is a likely precursor of the dominant acetyl radical observed. The presence of NO is well documented in tobacco smoke (Baren et al., 2004; Borgerding and Klus, 2005) with the accepted values typically 300 to 600 ppm or $1.7 \pm 0.2 \mu\text{g}/\text{cig}$ (Baren et al., 2004; Pryor et al., 1993). However, the concentration of NO_2 continues to be disputed (Shorter et al., 2006; Wooten, 2011).

Cueto and Pryor (1994) reported that nitric oxide disappeared as nitrogen dioxide appeared in tobacco smoke and in mixtures of nitric oxide, methanol, and isoprene in air (Cueto and Pryor, 1994). In contrast, Shorter and colleagues, using a very sensitive technique called quantum cascade tunable infrared laser differential absorption spectroscopy (TILDAS), detected very little NO_2 in mainstream cigarette smoke (Shorter et al., 2006).

Several important differences in the experiments can reconcile this discrepancy. Cueto and Pryor sampled undiluted smoke over a period of 800 s. In Shorter's experiment, the mainstream smoke was diluted by a factor of 4.2 before being drawn into the gas cell. The concentration was further decreased because the pressure in the sample cell was extremely low, about 0.059 atm. At this greatly reduced NO concentration NO-NO₂ conversion would be dramatically slowed. Thus very little NO₂ would be expected within the 0.16 s sampling period, and little was detected. An additional potential discrepancy for Cueto and Pryor is their practice of "conditioning" cigarettes over a supersaturated ammonium nitrate solution to maintain constant humidity (Cueto and Pryor, 1994); presumably this practice could increase the nitrogen content of the tobacco.

We started our simulation of reactions 1 and 2 by employing two sets of initial concentrations of acetaldehyde and nitric oxide corresponding to: (i) our experimental gas mixture, and (ii) literature data for 3R4F reference cigarette. In order to assess the maximum potential acetyl radical production with the simulations we used the maximum concentrations for all components, which occur at their mixing point, and high concentration of oxygen (equivalent to 21%). Modeling the dynamics of dilution as the pressure drops through the column was beyond the scope of this project. The initial concentration of acetaldehyde in the experimental gas mixture was very high because of its high vapor pressure (vapor pressure at 20 °C 98.65 kPa). In simulations an initial concentration of nearly 1 atm pressure was chosen for acetaldehyde by assuming that the liquid and vapor were in equilibrium at 20°C and NO was defined by the tank standard as 1000 ppm. The simulation was run for 8000 s to fully reproduce the rise and decrease of NO₂. To simulate cigarette smoke, the initial concentration for NO was similar while acetaldehyde was much lower, at realistic levels for smoke. Reaction 1 occurs with a third-order rate constant of $2.00 \times 10^{-38} \text{ cm}^6/\text{molecules}^2 \cdot \text{s}$ at 298K (Atkinson et al., 2004). Reactive NO₂, produced from relatively unreactive NO in smoke, can abstract H from CH₃CHO to produce CH₃C(O)· with a second-order rate constant of $3.36 \times 10^{-23} \text{ cm}^3/\text{molecules} \cdot \text{s}$ at 298K (Jaffe and Wan, 1974). A kinetic analysis using concentrations employed in our gas mixture reaction gives a plot of concentrations vs. time (shown in Figure 4(a)). As a first test of the mechanism feasibility the acetyl radical was generated and allowed to accumulate, neglecting scavenging reactions (e.g. CH₃C(O)· reacting with 3AP, NO₂ or O₂).

Figure 4(a) shows that NO₂ concentration increases in the first few minutes, reaching its maximum at about 300 s, and afterwards decreases because of the combined effects of depletion by acetaldehyde and the consumption of NO in the gas mixture. The NO/NO₂ simulated concentration shows a similar profile to the appearance and disappearance of NO/NO₂ measured by FT-IR in previous experiments (Cueto and Pryor, 1994). Acetyl radical concentration increases in the beginning and reaches a plateau several minutes later after all reactants are consumed. Based on this computational simulation, it is not a surprise that puff-resolved FTC generates more acetyl radical than the continuous method, for the puff-resolved FTC methods allow longer residence time (at least 60 s) than its counterpart (~ 10 s) for NO₂ to evolve in the smoke.

For a real-world cigarette smoke scenario, we take 3R4F Kentucky Reference cigarette under FTC standard smoking conditions as an example. Literature values for 2R4F (which

were replaced by the 3R4F series) were chosen for the initial concentrations of NO and acetaldehyde because the concentration data for 3R4F are not available. We expect the acetaldehyde concentration of 584 $\mu\text{g}/\text{cig}$ (mainstream smoke) to be similar (Lin and Yu, 2011). Based on an average of 8 puffs for each cigarette, there is 73 μg of acetaldehyde in each 35 mL puff, neglecting the loss from smoldering process. Hence, 2.85×10^{16} molecules/ cm^3 of acetaldehyde was used as the initial concentration for the smoke simulation (which is 850 times less than the model gas example). A similar calculation provided the initial nitrogen oxide concentration for the smoke simulation. The concentration of NO in mainstream smoke for a 2R4F cigarette is from 300 ppm to 600 ppm, which is 7.38×10^{15} to 1.61×10^{16} molecules/ cm^3 (Baren et al., 2004; Cueto and Pryor, 1994); a value of 1.35×10^{16} molecules/ cm^3 was selected, similar to the value for the model gas mixture.

As shown in Figure 4(b), the simulation gives a maximum accumulated concentration of 1.3 nmol/L $\text{CH}_3\text{CO}_3\cdot$ at 250 seconds, which is the longest residence time of FTC puff-resolved smoke in the column. The total of about 0.36 nmol for the 280 mL of smoke sampled for each cigarette is far less than the number trapped experimentally, 50–84 nmol/cigarette, from the 3R4F Kentucky Reference cigarette under FTC conditions. Thus, while acetyl radical generation by reactions of CH_3CHO and NO_2 is kinetically feasible, at plausible initial concentrations of these major components in tobacco smoke, these gas phase reactions cannot account for the amount of acetyl radical detected.

4.2 Atmospheric Chain Reactions Investigated with MCM

A series of chain reactions (Scheme 2 and Table 1) has the potential to increase the yield of acetyl radical; they can be simulated by the MCM program. In the presence of oxygen, acetyl radical is rapidly oxidized to acetyl peroxide radical, which accelerates the conversion of NO into NO_2 . The resulting $\text{RO}\cdot$ can produce $\text{HO}_2\cdot$, which can again convert NO into NO_2 and also generate an OH radical, which can abstract hydrogen from acetaldehyde with a rate constant 10^{12} times larger than that for hydrogen abstraction by NO_2 . Thus chain branching has the potential to increase production of acetyl radicals.

The MCM program is designed to simulate atmospheric reactions given selected initial species and, importantly, includes reactions of peroxide species resulting from addition of oxygen to primary radicals. Note that because oxygen concentrations are high, reactions of radicals with species other than O_2 (e.g. $\text{R}\cdot + \text{CO}$, $\text{R}\cdot + \text{CH}_3\text{COH}$) are insignificant.

In modeling these chain reaction mechanisms we must explicitly include the 3AP radical trap. Because the O_2 scavenging reaction is very fast ($k_4=5.00 \times 10^{-12} \text{cm}^3/\text{molecule s}$) and O_2 is present in high concentrations (5.26×10^{18} molecules/ cm^3), the steady state concentration of acetyl radical is extremely small. However, radical trapping schemes, with 3AP or nitron spin traps, do not measure steady state radical concentrations; rather they act as competitive scavengers for the radicals, removing a fraction from the chain process as depicted in Scheme 2(a). Through Branch I, acetyl radicals are trapped by 3AP and removed from the reaction cycle; through Branch II, the radicals react with oxygen to produce acetyl peroxide, which can ultimately regenerate acetyl radical through a series of chain reactions. Because 3AP and oxygen compete for acetyl radicals, the amount trapped by 3AP depends on the relative ratio of $k_{3\text{AP}}[3\text{AP}]/k_{\text{O}_2}[\text{O}_2]$. To simulate experimental results, we must

specify a trapping rate, i.e. $k_{3AP}[3AP]$, which is not well defined because 3AP is adsorbed to the surface. Increasing the surface area for trapping has been shown to increase the yield of trapped radicals, although it was not possible to out-compete oxygen (Flicker and Green, 2001). The initial concentrations employed in the MCM modeling are as given in Figure 4(b); 3AP was varied from 5.56×10^{10} to 5.56×10^{20} molecules/cm³ to study the trapping efficiency. The reactions and rate constants for this simulation are shown in Table 1. The simulation gives the concentration of CH₃O-3AP trapped in the first 25 seconds. Figure 5 shows MCM-based kinetic calculation of the production of CH₃C(O)· trapped by 3AP from the 3R4F Kentucky Reference cigarette smoke at 25 s when $k_{3AP}[3AP]/k_{O_2}[O_2]$ equals to 10^{-8} , 10^{-4} and 100 respectively.

Figure 6 shows that with increasing ratios $k_{3AP}[3AP]/k_{O_2}[O_2]$, the CH₃CO-3AP concentration at 25 s increases first and then starts to drop at certain a $k_{3AP}[3AP]/k_{O_2}[O_2]$ ratio, and in the end levels off when the ratio is larger than about 10^{-3} .

Figure 7 shows the relationship between the amount of acetyl radical trapped and the $k_{3AP}[3AP]/k_{O_2}[O_2]$ ratio. Surprisingly, the amount trapped does not increase continuously with increasing 3AP concentration. Instead, a peak occurs when $k_{3AP}[3AP]/k_{O_2}[O_2]$ equals 10^{-4} . At very small concentrations of 3AP most acetyl radicals react with O₂, and few are trapped; at high 3AP concentrations, all acetyl radicals are trapped as they are formed, thwarting the chain reactions and resulting in a maximum trapped amount equivalent to values calculated from the simplified Matlab model at 25 s, 0.0195 nmol/L (Fig. S5.). Between these extremes, the amount trapped is dictated by competition between 3AP and oxygen, and enhanced radical production through chain reactions. This effect is accentuated by the additional isoprene as discussed below.

4.3 Atmospheric Chain Reactions including Isoprene Investigated with MCM

An additional source of radicals could be unsaturated organic compounds such as isoprene, which is a major constituent of tobacco smoke (200–400 µg/cigarette) (Hoffmann et al., 2001). These compounds can undergo radical reactions to generate HO₂, which can refuel the generation of acetyl radical (Scheme 3).

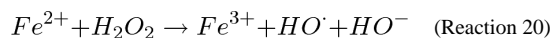
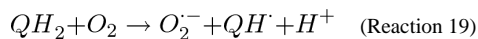
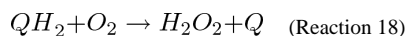
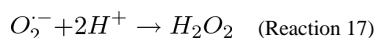
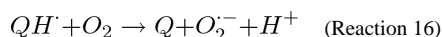
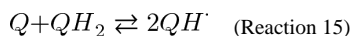
Including isoprene in the MCM model adds reactions 10–14 (Table 1) and accelerates production of peroxy and hydroxy radicals, as well as NO₂. Specifically, at 250 s, the levels of OH are over 10,000 times greater while the NO₂ concentration slightly increases (Figure S4). Adding isoprene-initiated reactions boosts the calculated yield of acetyl radicals to 3000 nmol/L, or 840 nmol/cigarette, when the $k_{3AP}[3AP]/k_{O_2}[O_2]$ ratio is 10 at 25 s. Lower ratios than 10 are probably more realistic and, according to the sensitivity shown in Figure 7, could easily produce the observed experimental range of 50–84 nmol/cigarette of acetyl radical from 3R4F research cigarettes under FTC standard smoking conditions (Bartalis et al., 2007; Bartalis et al., 2009; Gerardi and Coleman, 2010).

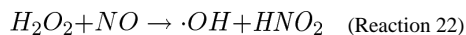
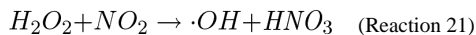
As shown in Figure 7, addition of isoprene has a strong effect on the amount of acetyl radical trapped by 3AP relative to oxygen. Models with and without isoprene both show peak trapping at specific $k_{3AP}[3AP]/k_{O_2}[O_2]$ ratios. In NO/air/CH₃CHO model, the highest concentration of CH₃CHO-3AP of 0.023 nmol/L is obtained when $k_{3AP}[3AP]/k_{O_2}[O_2]$ is

about 10^{-5} ; in NO/air/CH₃CHO/isoprene model, the highest concentration of CH₃CHO-3AP of more than 200 nmol/L is obtained when $k_{3AP}[3AP]/k_{O_2}[O_2]$ is about 10^{-2} . The shift of optimal $k_{3AP}[3AP]/k_{O_2}[O_2]$ in two different models is because many more acetyl radicals are generated by NO/air/CH₃CHO/isoprene model, thus more 3AP is required to trap them. Hence, the optimal $k_{3AP}[3AP]/k_{O_2}[O_2]$ increases from 10^{-4} to 10^{-2} in NO/air/CH₃CHO and NO/air/CH₃CHO/isoprene models.

A clear conclusion of Figure 7 is that the values of radicals trapped by nitroxides as often reported in the literature should not be considered definitive. Only a small fraction of radicals are trapped, and trapping interrupts further radical generation. Based on different models or reactions, different optimal ratios are suggested. Indeed, in a dynamic system where radicals are continually generated and consumed, the concept of radicals/cigarette isn't well defined and does not provide the full profile of radical generation in gas phase cigarette smoke. Thus, although to remain consistent with previous studies we have reported radical numbers in units of nmol/cigarette and nmol/L, these units are only appropriate to compare results of similar experiments. In addition to acetaldehyde and isoprene, the numerous other aldehydes and alkenes in tobacco smoke, although present at lower concentrations than these dominant species, undoubtedly undergo similar reactions to generate acetyl radicals in tobacco smoke. Furthermore, these chain reactions provide a mechanism to explain other radical species detected in smoke through reactions of hydroxyl and peroxy radicals with other smoke constituents.

The synergistic effect of tobacco tar is likely to be another source for the radicals measured in gas phase smoke. Long-lived reactive radicals are well-documented on tobacco tar (Maskos et al., 2008; Pryor et al., 1983a; Pryor et al., 1983b). The TPM accumulated on the filter provides tar-deposited long-lived radicals such as semiquinone (QH·), derived from reduction or oxidation of quinones (Q) or hydroquinones (QH₂), respectively, and which can produce superoxide anion (O₂⁻) and subsequently H₂O₂ and the reactive hydroxyl radical (HO·) as shown in Reaction 15–22 below (Valavanidis et al., 2009).





Reactions 15–22 provide an additional heterogeneous source of radicals that cannot be easily modeled.

5. Conclusions

Computational simulations using Matlab and the Master Chemical Mechanism demonstrated that although acetyl radical generation from reactions of CH₃CHO and NO/NO₂ and subsequent chain reactions is feasible, the concentrations of these species in gas phase tobacco smoke cannot account for the amount of acetyl radical detected. However, the addition of isoprene promotes the generation of sufficient hydroxyl and peroxy radicals to accelerate radical generation and accounts for the full amount of acetyl radical detected experimentally.

Simulations also showed that trapping techniques are very sensitive to the relative rates of reaction with the trapping species, 3AP, and oxygen; thus small variations in their concentrations can dramatically change the amount of radical trapped. Caution is advised in comparing numbers of radicals determined from different experiments. The application of the atmospheric model MCM to tobacco smoke has been demonstrated as a promising approach to unraveling the evolution of reactive species in smoke.

Supplementary Material

Refer to Web version on PubMed Central for supplementary material.

Acknowledgments

Grant Support: The authors gratefully acknowledge the support from the National Institute on Drug Abuse (NIDA), under National Institutes of Health contract 1R01DA17201.

References

- Atkinson R, Baulch DL, Cox RA, Crowley JN, Hampson RF, Hynes RG, Jenkin ME, Rossi MJ, Troe J. Evaluated kinetic and photochemical data for atmospheric chemistry: Volume I - gas phase reactions of Ox, HOx, NOx and SOx species. *Atmos Chem Phys*. 2004; 4:1461–1738.
- Atkinson R, Baulch DL, Cox RA, Hampson RF, Kerr JA, Rossi MJ, Troe J. Evaluated kinetic, photochemical and heterogeneous data for atmospheric chemistry. 5. IUPAC Subcommittee on Gas Kinetic Data Evaluation for Atmospheric Chemistry. *J Phys Chem Ref Data*. 1997; 26:521–1011.
- Atkinson R, Baulch DL, Cox RA, Crowley JN, Hampson RF, Hynes RG, Jenkin ME, Rossi MJ, Troe J. IUPAC Subcommittee. Evaluated kinetic and photochemical data for atmospheric chemistry: Volume II – gas phase reactions of organic species. *Atmos Chem Phys*. 2006; 6:3625–4055.
- Baker, R. Tobacco: production, chemistry, and technology. Blackwell Science; 1999. p. 398-439.
- Baren RE, Parrish ME, Shafer KH, Harward CN, Quan S, Nelson DD, McManus JB, Zahniser MS. Quad quantum cascade laser spectrometer with dual gas cells for the simultaneous analysis of mainstream and sidestream cigarette smoke. *Spectrochim Acta A*. 2004; 60:3437–3447.

- Bartalis J, Chan WG, Wooten JB. A new look at radicals in cigarette smoke. *Anal Chem.* 2007; 79:5103–5106. [PubMed: 17530742]
- Bartalis J, Zhao YL, Flora JW, Paine JB, Wooten JB. Carbon-centered radicals in cigarette smoke: acyl and alkylaminocarbonyl radicals. *Anal Chem.* 2009; 81:631–641. [PubMed: 19093757]
- Borgerding M, Klus H. Analysis of complex mixtures - Cigarette smoke. *Experimental and Toxicologic Pathology.* 2005; 57:43–73. [PubMed: 16092717]
- Brook, D. [accessed 6 Nov. 2010] Reaction object from online Matlab user library. 2005. Available: <http://www.mathworks.com/matlabcentral/fileexchange/7821-reaction-object/>
- Cueto R, Pryor WA. Cigarette-Smoke Chemistry - Conversion of Nitric-Oxide to Nitrogen-Dioxide and Reactions of Nitrogen-Oxides with Other Smoke Components as Studied by Fourier-Transform Infrared-Spectroscopy. *Vib Spectrosc.* 1994; 7:97–111.
- Davies, MH.; Vaught, A. *The Reference Cigarette.* Kentucky Tobacco Research and Development Center; University of Kentucky; Lexington, KY: 1990.
- ERI. [accessed 6 Nov. 2010] Eigenvector Research Incorporated Dataset. 2010. Available: <http://www.eigenvector.com/>
- Flicker TM, Green SA. Detection and separation of gas-phase carbon-centered radicals from cigarette smoke and diesel exhaust. *Analytical Chemistry.* 1998; 70:2008–2012. [PubMed: 21651292]
- Flicker TM, Green SA. Comparison of gas-phase free-radical populations in tobacco smoke and model systems by HPLC. *Environ Health Perspect.* 2001; 109:765–771. [PubMed: 11564610]
- Gerardi AR, Coleman WM. New Methodologies for Qualitative and Semi-Quantitative Determination of Carbon-Centered Free Radicals in Cigarette Smoke Using Liquid Chromatography-Tandem Mass Spectrometry and Gas Chromatography-Mass Selective Detection. *Beiträge zur Tabakforschung International/Contributions to Tobacco Research.* 2010; 24:58–71.
- Hoffmann D, Hoffmann I, El-Bayoumy K. The less harmful cigarette: a controversial issue. a tribute to Ernst L. Wynder. *Chem Res Toxicol.* 2001; 14:767–790. [PubMed: 11453723]
- Huang MF, Lin WL, Ma YC. A study of reactive oxygen species in mainstream of cigarette. *Indoor Air.* 2005; 15:135–140. [PubMed: 15737156]
- Jaffe S, Wan E. Thermal and Photochemical Reactions of NO₂ with Butyraldehyde in Gas-Phase. *Environmental Science & Technology.* 1974; 8:1024–1025.
- Jia M, Tang Y, Lam YF, Green SA, Blough NV. Prefluorescent Nitroxide Probe for the Highly Sensitive Determination of Peroxyl and Other Radical Oxidants. *Analytical Chemistry.* 2009; 81:8033–8040. [PubMed: 19788316]
- Lin P, Yu JZ. Generation of Reactive Oxygen Species Mediated by Humic-like Substances in Atmospheric Aerosols. *Environmental Science & Technology.* 2011; 45:10362–10368. [PubMed: 22044074]
- Lyons MJ, Gibson JF, Ingram DJ. Free-radicals produced in cigarette smoke. *Nature.* 1958; 181:1003–1004. [PubMed: 13541350]
- Maskos Z, Khachatryan L, Dellinger B. Formation of the persistent primary radicals from the pyrolysis of tobacco. *Energ Fuel.* 2008; 22:1027–1033.
- Orlando JJ, Tyndall GS, Wallington TJ. The atmospheric chemistry of alkoxy radicals. *Chem Rev.* 2003; 103:4657–4690. [PubMed: 14664628]
- Ozguner F, Koyu A, Cesur G. Active smoking causes oxidative stress and decreases blood melatonin levels. *Toxicol Ind Health.* 2005; 21:21–26. [PubMed: 15986573]
- Pandis, SN.; Seinfeld, JH. *Atmospheric Chemistry and Physics.* 1998.
- Paulson SE, Flagan RC, Seinfeld JH. Atmospheric Photooxidation of Isoprene. 1. The Hydroxyl Radical and Ground-State Atomic Oxygen Reactions. *Int J Chem Kinet.* 1992; 24:79–101.
- Polzin GM, Kosa-Maines RE, Ashley DL, Watson CH. Analysis of volatile organic compounds in mainstream cigarette smoke. *Environmental Science & Technology.* 2007; 41:1297–1302. [PubMed: 17593733]
- Pryor WA. Cancer and free radicals. *Basic Life Sci.* 1986; 39:45–59. [PubMed: 3767848]
- Pryor WA, Hales BJ, Premovic PI, Church DF. The radicals in cigarette tar: their nature and suggested physiological implications. *Science.* 1983a; 220:425–427. [PubMed: 6301009]

- Pryor WA, Prier DG, Church DF. Electron-Spin Resonance Study of Mainstream and Sidestream Cigarette-Smoke - Nature of the Free-Radicals in Gas-Phase Smoke and in Cigarette Tar. *Environ Health Persp.* 1983b; 47:345–355.
- Pryor WA, Stone K, Stone K, Cross CE, Machlin L, Packer L. Oxidants in Cigarette-Smoke - Radicals, Hydrogen-Peroxide, Peroxynitrate, and Peroxynitrite. *Ann NY Acad Sci.* 1993; 686:12–28. [PubMed: 8512242]
- Saunders SM, Jenkin ME, Derwent RG, Pilling MJ. World Wide Web site of a Master Chemical Mechanism (MCM) for use in tropospheric chemistry models. *Atmos Environ.* 1997; 31:1249–1249.
- Saunders SM, Jenkin ME, Derwent RG, Pilling MJ. Protocol for the development of the Master Chemical Mechanism, MCM v3 (Part A): tropospheric degradation of non-aromatic volatile organic compounds. *Atmos Chem Phys.* 2003; 3:161–180.
- Shorter JH, Nelson DD, Zahniser MS, Parrish ME, Crawford DR, Gee DL. Measurement of nitrogen dioxide in cigarette smoke using quantum cascade tunable infrared laser differential absorption spectroscopy (TILDAS). *Spectrochim Acta A.* 2006; 63:994–1001.
- Stabbert R, Schafer KH, Biefel C, Rustemeier K. Analysis of aromatic amines in cigarette smoke. *Rapid Commun Mass Sp.* 2003a; 17:2125–2132.
- Stabbert R, Voncken P, Rustemeier K, Haussmann HJ, Roemer E, Schaffernicht H, Patskan G. Toxicological evaluation of an electrically heated cigarette. Part 2: Chemical composition of mainstream smoke. *J Appl Toxicol.* 2003b; 23:329–339. [PubMed: 12975772]
- Thompson BT, Mizaikoff B. Real-time Fourier transform-infrared analysis of carbon monoxide and nitric oxide in sidestream cigarette smoke. *Applied Spectroscopy.* 2006; 60:272–278. [PubMed: 16608570]
- Valavanidis A, Vlachogianni T, Fiotakis K. Tobacco smoke: involvement of reactive oxygen species and stable free radicals in mechanisms of oxidative damage, carcinogenesis and synergistic effects with other respirable particles. *Int J Environ Res Public Health.* 2009; 6:445–462. [PubMed: 19440393]
- Wooten JB. Gas-phase Radicals in Cigarette Smoke: A Re-evaluation of the Steady-State Model and the Cambridge Filter Pad. *Mini-Reviews in Organic Chemistry.* 2011; 8:412–426.

Highlights

- Acetyl radicals were measured in tobacco smoke and model gas mixtures.
- Mechanisms and kinetics of NO-initiated radical formation were simulated.
- Acetyl radicals originate from acetaldehyde in tobacco smoke.
- Chain reactions with isoprene and oxygen can produce observed acetyl radical levels.

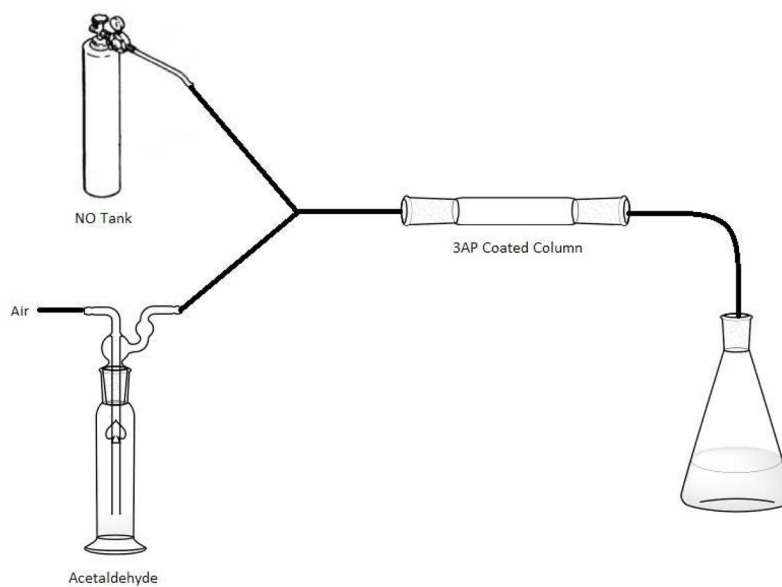
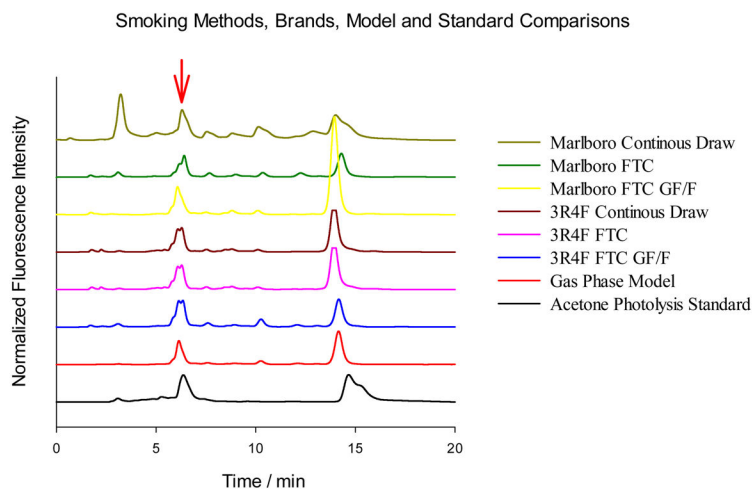
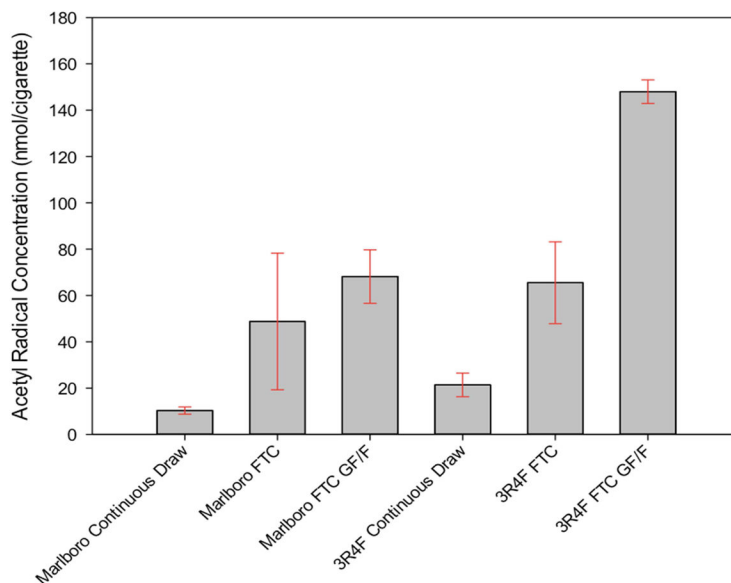


Figure 1. Diagram of the gas mixture reaction apparatus. Tubing was Teflon with glass connectors.



(a)



(b)

Figure 2.

(a). Representative normalized chromatograms of radicals trapped from fresh cigarette smokes, model gas mixture, and photolyzed aqueous acetone sample. All samples included the radical trap (3AP) and were derivatized with NDA. NDA-3AP-C(O)CH₃ elutes at around 6.3 min, as indicated by the red arrow. HPLC conditions are given in experimental section. (b). Acetyl radical concentrations compared for different cigarettes types, smoking conditions and particle filter set up. Error bars on the column diagram represent standard deviations of three replicates.

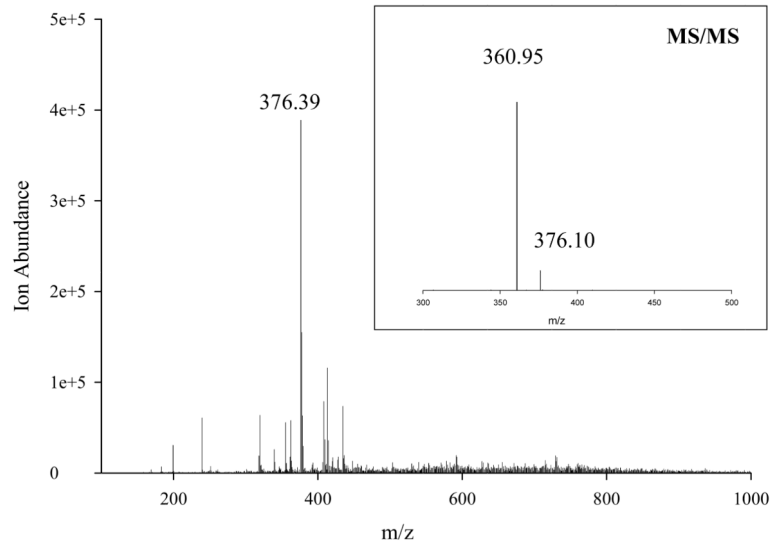
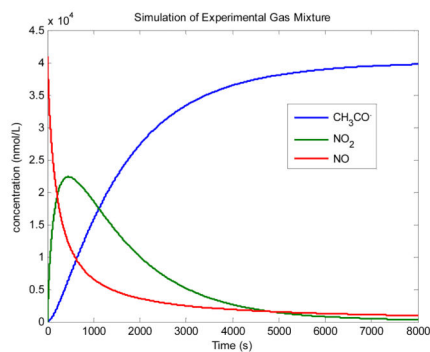
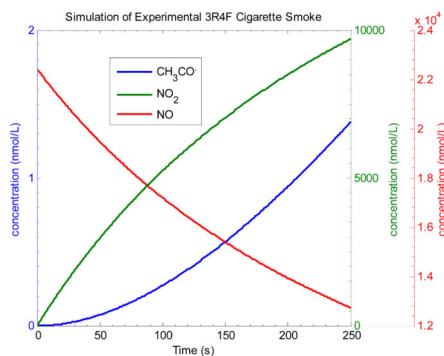


Figure 3. Left: ESI-MS spectrum of R-3AP-NDA adduct of the Marlboro smoke sample with m/z range of 100–1000; Insert: MS/MS of m/z 376.4 by CID.



(a)



(b)

Figure 4.

(a). Model mixture simulation. $[\text{NO}]_0 = 2.47 \times 10^{16}$ molecules/cm³; $[\text{CH}_3\text{CHO}]_0 = 2.44 \times 10^{19}$ molecules/cm³; $[\text{O}_2]_0 = 5.26 \times 10^{18}$ molecules/cm³. (b). 3R4F Kentucky Reference cigarette smoke simulation, based on initial concentrations of CH₃CHO and NO from literature sources. $[\text{NO}]_0 = 1.35 \times 10^{16}$ molecules/cm³; $[\text{CH}_3\text{CHO}]_0 = 2.85 \times 10^{16}$ molecules/cm³; $[\text{O}_2]_0 = 5.26 \times 10^{18}$ molecules/cm³.

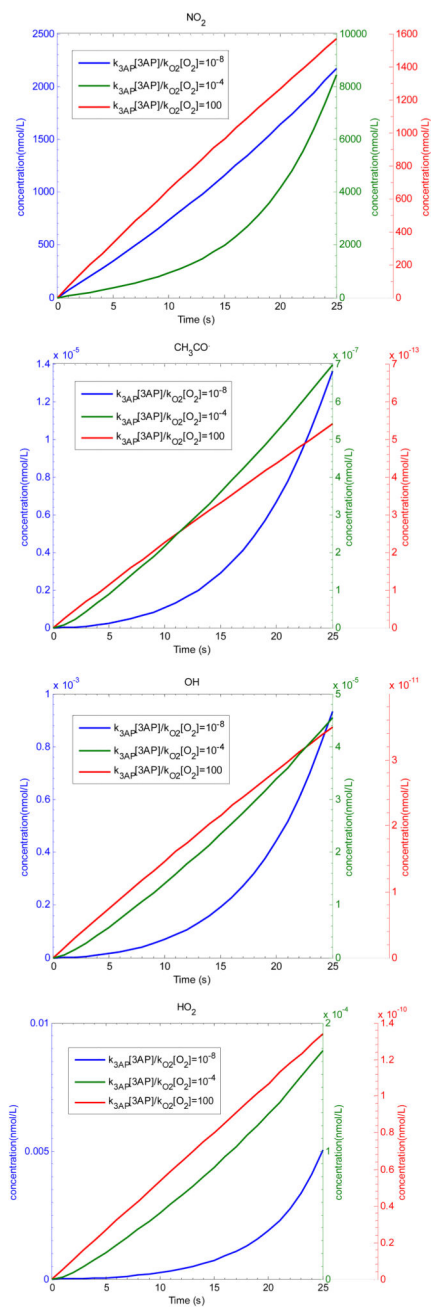


Figure 5. MCM simulation on NO₂, CH₃CO, OH and HO₂ concentrations by NO/air/CH₃CHO model from the 3R4F Kentucky Reference cigarette smoke at 25 s when $k_{3AP}[3AP]/k_{O_2}[O_2]$ equals to 10^{-8} , 10^{-4} and 100.

Competitive Effects of 3AP and O₂
on Acetyl Radical Trapping by NO/air/CH₃CHO Model

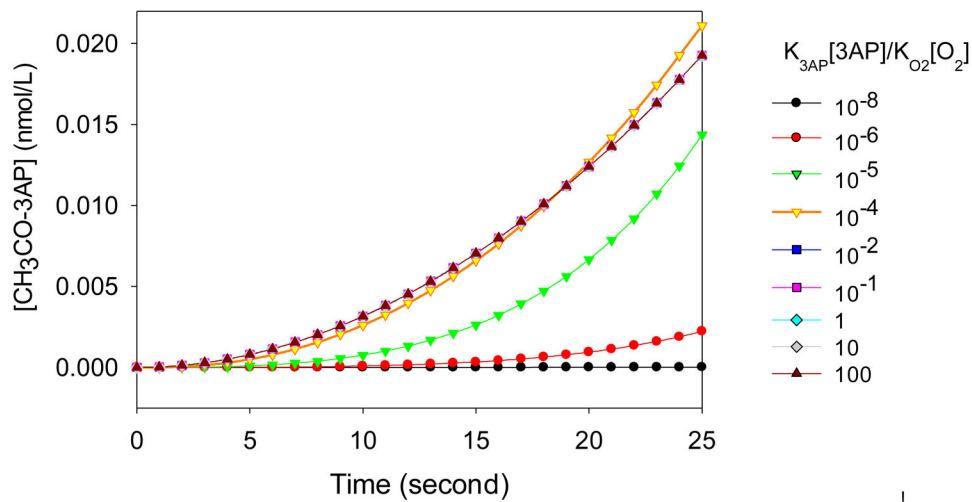


Figure 6. MCM simulation by NO/air/CH₃CHO model on the generation of CH₃C(O)-3AP at different $k_{3AP}[3AP]/k_{O_2}[O_2]$.

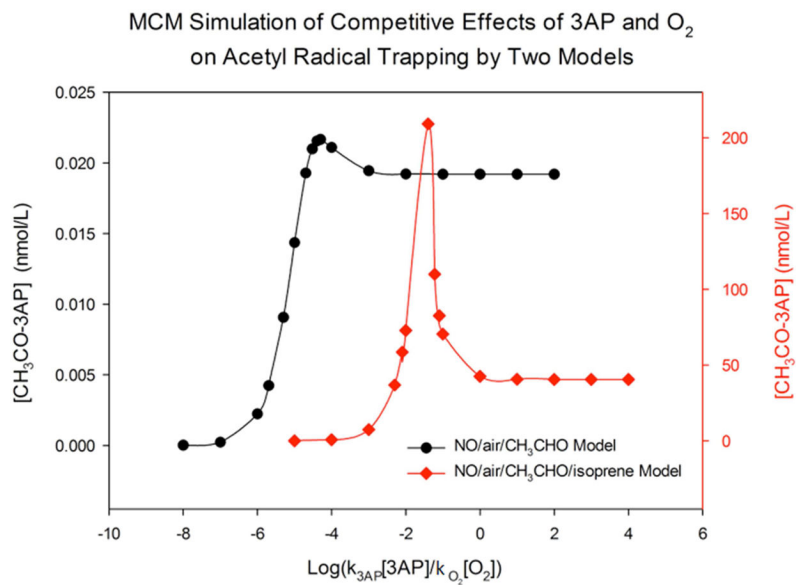
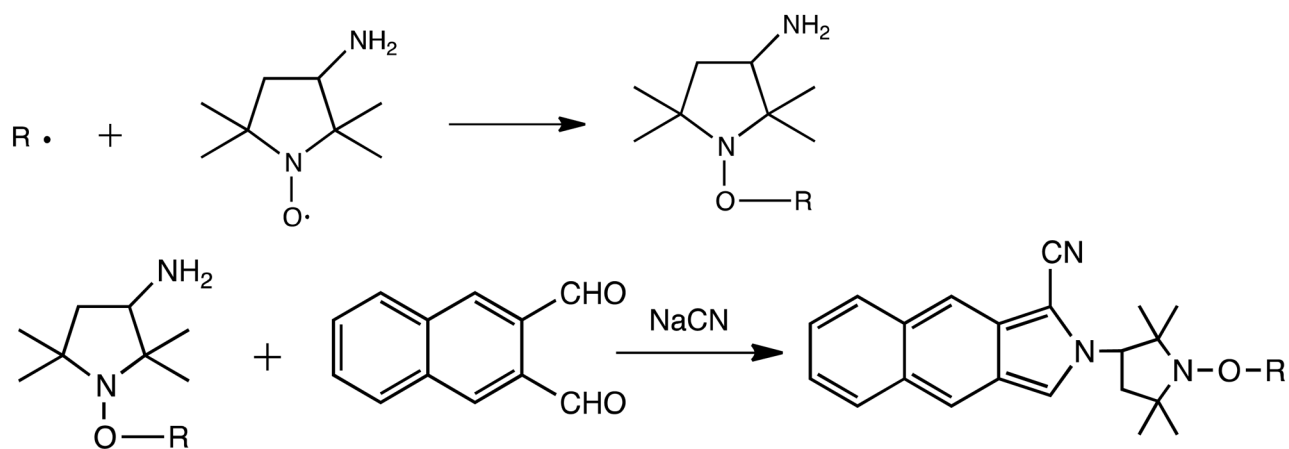
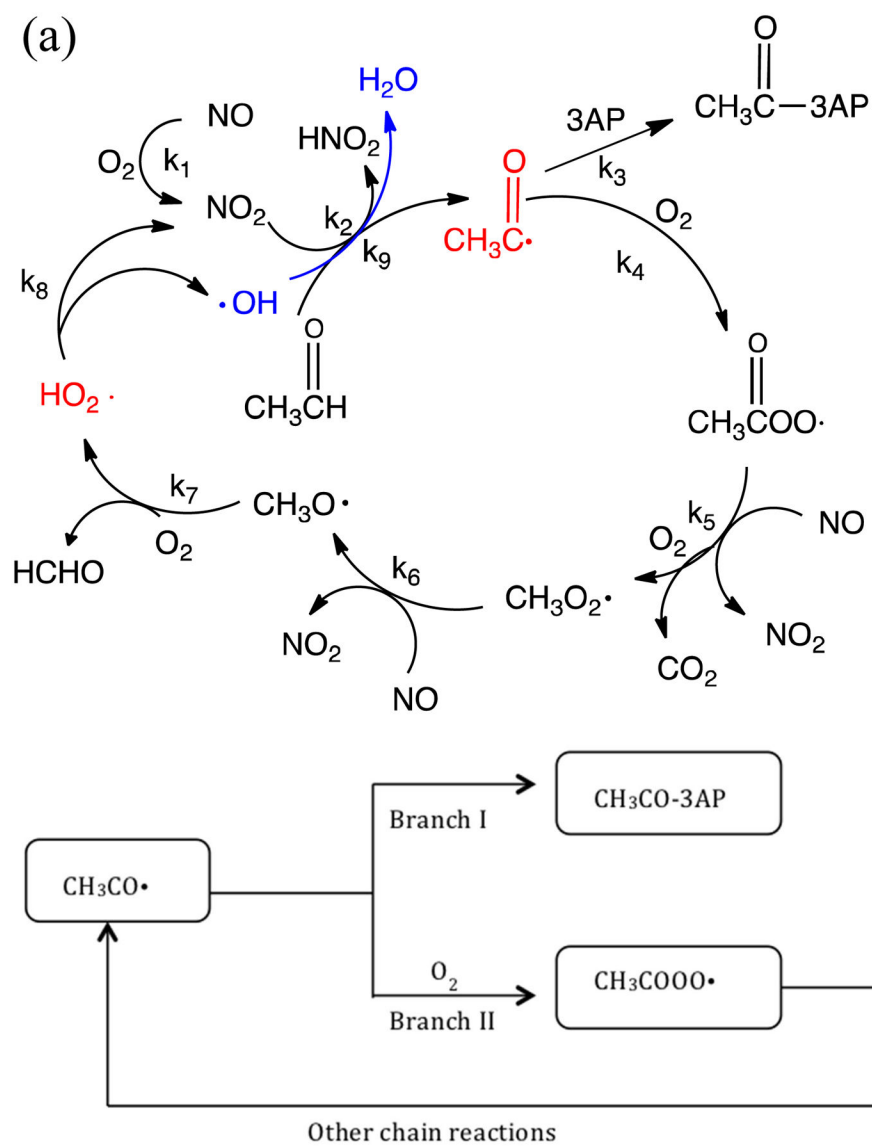


Figure 7. Comparison of the competitive effects of 3AP and O₂ on acetyl radical trapping by NO/air/CH₃CHO and NO/air/CH₃CHO/isoprene models.

**Scheme 1.**

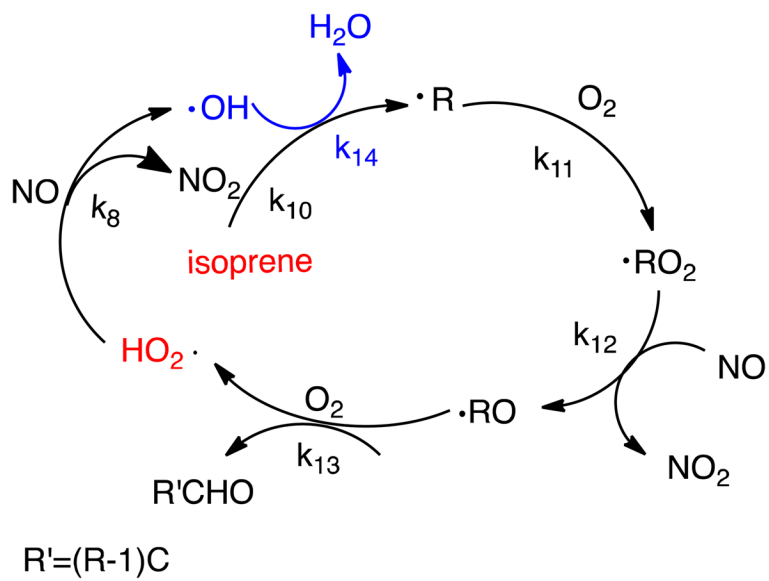
Trapping of carbon-centered radical ($\cdot R$) by 3AP, followed by solution-phase derivatization with NDA to produce the fluorescent radical-adduct.



(b)

Scheme 2.

(a). Acetaldehyde-based chain reactions of acetyl radical generation in tobacco smoke. (b). The flowchart of acetyl radical cycling and sinks in gas phase.

**Scheme 3.**

Isoprene chain reactions to generate HO₂ radical in gas phase smoke.

Table 1

Proposed reactions for acetyl radical generation in tobacco smoke.

No.	Reaction	Reaction rate constants ^d
1	$2NO + O_2 \rightarrow 2NO_2$	$k_1 = 2.0 \times 10^{-38}$
2	$CH_3CHO + NO_2 \rightarrow CH_3C(O) \cdot + HNO_2$	$k_2 = 3.36 \times 10^{-23}$
3	$CH_3C(O) \cdot + 3AP \rightarrow CH_3C(O) - 3AP$	$k_3 = 5.00 \times 10^{-12}$
4	$CH_3C(O) \cdot + O_2 \rightarrow CH_3C(O)O_2 \cdot$	$k_4 = 5.00 \times 10^{-12}$
5	$CH_3C(O)O_2 \cdot + NO + O_2 \rightarrow CH_3O_2 \cdot + NO_2 + CO_2$	$k_5 = 2.4 \times 10^{-11}$
6	$CH_3O_2 \cdot + NO \rightarrow CH_3O \cdot + NO_2$	$k_6 = 8.9 \times 10^{-12}$
7	$CH_3O \cdot + O_2 \rightarrow HCHO + HO_2 \cdot$	$k_7 = 1.65 \times 10^{-15}$
8	$HO_2 \cdot + NO \rightarrow NO_2 + OH \cdot$	$k_8 = 8.91 \times 10^{-12}$
9	$CH_3CHO + OH \cdot \rightarrow CH_3C(O) \cdot + H_2O$	$k_9 = 1.50 \times 10^{-11}$
10	$NO_2 + C_5H_8 \rightarrow R \cdot$	$k_{10}^b = 1.81 \times 10^{-19}$
11	$R \cdot + O_2 \rightarrow RO_2 \cdot$	$k_{11} = 5.00 \times 10^{-12}$
12	$RO_2 \cdot + NO \rightarrow RO \cdot + NO_2$	$k_{12} = 8.9 \times 10^{-12}$
13	$RO \cdot + O_2 \rightarrow R'CHO + HO_2 \cdot$	$k_{13} = 1.9 \times 10^{-15}$
14	$C_5H_8 + OH \cdot \rightarrow R \cdot$	$k_{14}^c = 1.01 \times 10^{-15}$

^aUnits for second order rate constants: cm³/molecule s;Third order third rate constants: cm⁶/molecule² s; all rate constants for 298 K. (Atkinson et al., 2004; Atkinson et al., 1997; Atkinson, et al., 2006; Jaffe and Wan, 1974; Orlando et al., 2003; Pandis, 1998; Paulson et al., 1992)^{b,c}R = C₅H₈-NO₂ or C₅H₈-OH